



Defence Research and
Development Canada

Recherche et développement
pour la défense Canada



Validation of the electromagnetic code FACETS for numerical simulation of radar target images

S. Wong

Defence R&D Canada – Ottawa

Technical Memorandum
DRDC Ottawa TM 2009-275
December 2009

Canada

Validation of the electromagnetic code FACETS for numerical simulation of radar target images

S. Wong
DRDC Ottawa

Defence R&D Canada – Ottawa

Technical Memorandum
DRDC Ottawa TM 2009-275
December 2009

Principal Author

Original signed by S. Wong

S. Wong
Defence Scientist

Approved by

Original signed by C. Wilcox

C. Wilcox
Section Head/RAST

Approved for release by

Original signed by B. Eatock

B. Eatock
Chief Scientist

- © Her Majesty the Queen in Right of Canada, as represented by the Minister of National Defence, 2009
- © Sa Majesté la Reine (en droit du Canada), telle que représentée par le ministre de la Défense nationale, 2009

Abstract

Validation of the computational electromagnetic code FACETS (Frequency Asymptotic Code for Electromagnetic Target Scattering) for simulating radar images of a target is obtained, through direct simulation-to-measurement comparisons. A 3-dimensional computer-aided design model of a canonical target known as SLICY (Sandia laboratory Implementation of Cylinders) and the corresponding measured SAR (Synthetic Aperture Radar) image data of SLICY from the MSTAR (Moving and Stationary Target Acquisition and Recognition) datasets are used in the validation process. Computed SAR images of the SLICY target sampled over 360 degrees in azimuth and at two elevation angles are evaluated by comparing against measured images. The results indicate that computed images of high fidelity can be generated if the scattering primitives on the target are correctly included in the computer-aided design model and this information is correctly translated for computation in the electromagnetic code.

Résumé

Pour valider le Frequency Asymptotic Code for Electromagnetic Target Scattering (FACETS [code de fréquence asymptotique pour la diffusion de cibles électromagnétiques]) du code électromagnétique computationnel aux fins de simulations d'images radar d'une cible, il faut comparer directement les résultats des simulations aux mesures. Un modèle tridimensionnel conçu par ordinateur d'une cible canonique, appelé Sandia Laboratory Implementation of Cylinders (SLICY [mise en place des cylindres du laboratoire Sandia]) et les données mesurées correspondantes des images du radar à synthèse d'ouverture (SAR) du SLICY provenant des ensembles de données de Moving and Stationary Target Acquisition and Recognition (MSTAR [acquisition et reconnaissance de cibles mobiles et fixes]) sont utilisés dans le processus de validation. Les images SAR calculées de la cible SLICY échantillonnée sur 360 degrés en azimuth et à deux angles de site sont comparées, aux fins d'évaluation, aux images mesurées. Selon les résultats, il est possible de produire des images calculées de haute fidélité si les primitives de diffusion sur la cible sont incorporées correctement au modèle conçu par ordinateur et si ces informations sont traduites correctement aux fins de calcul dans le code électromagnétique.

This page intentionally left blank.

Executive summary

Validation of the electromagnetic code FACETS for numerical simulation of radar target images

S. Wong; DRDC Ottawa TM 2009-275; Defence R&D Canada – Ottawa;
December 2009.

Introduction or background: Achieving accurate computational electromagnetic modeling (CEM) for generating synthetic target signatures in the radar domain has always been a big challenge. Validation of model simulated results against measurement on benchmark models has been a goal in the CEM community for quite some time. This is especially true in the defence science community where methods for validating simulated radar images of complex military targets such as aircraft, ships and ground vehicles with a consistent level of accuracy are highly sought. Simulated SAR (Synthetic Aperture Radar) images can be used in various applications, such as target database compilation in Non-Cooperative Target Recognition (NCTR) for Combat ID in naval air-defence, training human operators in assisted ISR (Intelligence, Surveillance and Reconnaissance) image analysis and analyzing stealth target images.

Proper methodology to assess an electromagnetic code can lead to valuable insights in identifying some of the problems encountered in radar target image simulation and prospective solutions to resolve these problems. A reasonable and logical approach to proper CEM validation is to have a well-defined target model as a benchmark reference for measurements. This benchmark target can also be represented by a 3-dimensional computer-aided design (CAD) model for numerical simulation. A target composed of scattering primitives such as flat surface, cylinder, dihedral, trihedral, and elementary cavity provides a well-defined reference. Such a canonical target allows researchers to gain a better understanding of the inner workings of the electromagnetic code's algorithm.

The objective of this work is to establish a better understanding of the process of radar image simulation using an electromagnetic code. In particular, radar target images in the X-band region around 10 GHz are of considerable interest; most military maritime and air-borne radar systems operate in this frequency region. A commercial electromagnetic code, FACETS (Frequency Asymptotic Code for Electromagnetic Target Scattering) is used for assessing the numerical simulation process. FACETS employs a "shooting-and-bouncing-ray" method that is especially well suited for radar image simulation of targets in the X-band radar frequency. This numerical method permits computation of a complex-target image to be done within a reasonable amount of computational time. Measured X-band image data of a canonical target known as SLICY (Sandia Laboratory Implementation of Cylinders) in the MSTAR (Moving and Stationary Targets Acquisition and Recognition) are used as a benchmark reference for comparing with the simulated target images. A direct comparison between simulated SAR images and measured data provides a sound basis for the validation of the FACETS code.

Results: Based on the canonical target SLICY with well-defined scattering primitives, the results from this work have indicated that synthetic target images of reasonably good fidelity can be generated if two requirements are met. These are:

1. The CAD model of the target must provide a reasonably accurate physical representation of the scattering primitives at the correct locations on the target.
2. The electromagnetic code must properly interpret the information given by the CAD model in computing the scattering primitives.

Although these requirements may seem obvious and trivial statements, it is not clear that these conditions can be met in a routine manner for a complex target. It has been found from past research work that there is no known procedure to ensure and to confirm that all pertinent scattering primitives relevant to the computational scattering processes are present and accurately constructed in the CAD model of a particular target. The study conducted in this work has verified that these are the minimum requirements needed for accurate target signature generation.

It is also found from the results of the SAR image simulation that diffraction effects from a target do not have a prominent contribution to the overall image of the target. They can be considered as second order effects comparing to double-bounce and triple-bounce scattering processes.

Significance: The analysis conducted in this work provides a convincing, direct SAR image simulation-to-measurement validation of the FACETS code. The results have shown that FACETS has the functionality to compute appropriately the basic scattering processes, provided that the electromagnetic code is prepared properly in handling the input information. This provides a useful framework as guideline for our continuing effort in the numerical simulation of radar target images.

Future plans: A continuing research effort is currently underway to extend the validation of FACETS to a real-world complex target. Attempts are being made to validate the computed SAR images of a self-propelled howitzer, the Gvozdika 2S1. The 2S1 self-propelled howitzer is chosen because a large portion of the target has a relatively “clean” shape with well-defined surfaces. Moreover, measured SAR images of the 2S1 self-propelled howitzer with accurate ground-truths are available for comparison from the MSTAR datasets.

Sommaire

Validation of the electromagnetic code FACETS for numerical simulation of radar target images

S. Wong; DRDC Ottawa TM 2009-275; R & D pour la défense Canada – Ottawa; Décembre 2009.

Introduction ou contexte: Dans le domaine du radar, l'obtention d'une modélisation électromagnétique computationnelle (CEM) précise en vue de produire des signatures de cibles synthétiques a toujours été un défi important. Depuis longtemps, l'un des objectifs de la communauté de la CEM est de valider des résultats de modèles simulés par rapport aux mesures prises sur des modèles de référence. Cet objectif est très présent dans la communauté scientifique de la Défense, qui désire fortement obtenir des méthodes de validation des images radars simulées de cibles militaires complexes, comme des aéronefs, des navires et des véhicules terrestres, dont le niveau de précision est constant. On peut en outre utiliser des images SAR simulées pour diverses applications, comme la compilation de base de données sur les cibles afin d'effectuer la reconnaissance de cible non coopérative (NCTR) aux fins d'identification au combat dans la défense aérienne navale, la formation d'opérateurs humains en analyse assistée d'images de renseignement, de surveillance et de reconnaissance (RSR), et l'analyse d'images de cibles furtives.

Une méthode appropriée d'évaluation d'un code électromagnétique permet d'obtenir des informations utiles sur le repérage de certains problèmes rencontrés dans la simulation d'images de cibles radar et leurs solutions potentielles. Une approche raisonnable et logique à la bonne validation CEM consiste à utiliser un modèle de cible bien défini comme référence pour les mesures. Cette cible de référence peut aussi être représentée par un modèle tridimensionnel conçu par ordinateur aux fins de simulation numérique. Une cible composée de primitives de diffusion, comme une surface plane, un cylindre, un dièdre, un trièdre et une cavité élémentaire, fournit une référence bien définie. Grâce à une cible canonique de ce genre, les chercheurs peuvent mieux comprendre le fonctionnement interne de l'algorithme du code électromagnétique.

Le présent travail vise à mieux comprendre le processus de simulation d'images radar au moyen d'un code électromagnétique. Notamment, les images de cibles radar dans la région de la bande X à une fréquence d'environ 10 GHz sont d'un grand intérêt, car la plupart des systèmes radar maritimes et aéroportés militaires fonctionnent dans cette zone de fréquences. Un code électromagnétique commercial, le FACETS, sert à évaluer le processus de simulation numérique. Le FACETS utilise une méthode de « rayon de lancer et de rebond » particulièrement bien adaptée à la simulation d'images radar de cible dans la fréquence radar en bande X. Cette méthode numérique permet de calculer une image d'une cible complexe dans un délai raisonnable. De plus, les données mesurées de l'image dans la bande X d'une cible canonique, appelées SLICY, dans MSTAR servent de référence pour comparer les images de cibles simulées. Une comparaison directe entre des images SAR simulées et des données mesurées fournit une base solide pour la validation du FACETS.

Résultats: À partir de la cible canonique SLICY dotée de primitives de diffusion bien définies, les résultats des présents travaux montrent que l'on peut produire des images de cibles synthétiques assez fiables si deux exigences sont respectées, soit :

1. le modèle conçu par ordinateur de la cible doit fournir une représentation physique assez précise des primitives de diffusion aux bons endroits sur la cible;
2. le code électromagnétique doit permettre d'interpréter correctement les informations fournies par les modèles conçus par ordinateur dans le calcul des primitives de diffusion.

Bien que ces exigences puissent sembler évidentes et banales, pour une cible complexe, on ne peut pas clairement affirmer qu'elles puissent être respectées sur une base régulière. Des travaux de recherches antérieurs ont montré qu'aucune procédure connue ne permet d'assurer ni de confirmer la présence de toutes les primitives de diffusion pertinentes liées aux processus de diffusion calculée et leur construction précise dans le modèle conçu par ordinateur d'une cible donnée. L'étude menée dans le cadre des présents travaux a permis de vérifier que ces énoncés sont les exigences minimales nécessaires pour la production de signatures de cibles précises.

Selon les résultats de la simulation d'images SAR, l'effet de diffraction d'une cible influe peu sur l'image globale de la cible. On considère qu'il s'agit d'effet de second ordre par rapport aux méthodes de diffusion à double réflexion et à triple réflexion.

Importance: L'analyse réalisée dans le cadre de s présents tr avaux a per mis de valider de façon directe et convaincante des résultats de simulation par rapport aux mesures d'images SAR du FACETS. Selon les résultats, le FACETS permet de calculer correctement les processus de diffusion de base, à condition que le code électromagnétique permette bien de manipuler les informations d'entrée. On obtient ainsi un cadre utile qui permet d'orienter nos efforts continus liés à la simulation numérique d'images de cibles radar.

Perspectives: Des recherches en cours visent à étendre la validation du FACETS aux cibles complexes réelles. On essaie de valider les images SAR calculées d'un obusier automoteur, Gvozdika 2S1. Cet obusier a été choisi parce qu'une grande partie de la cible a une forme relativement « propre » ainsi que des surfaces bien définies. De plus, les images SAR mesurées de l'obusier automoteur 2S1 dotées d'une réalité de terrain précise sont disponibles aux fins de comparaison dans les ensembles de données de MSTAR.

Table of contents

Abstract	i
Résumé	i
Executive summary	iii
Sommaire	v
Table of contents	vii
List of figures	viii
1 Introduction.....	1
2 Generation of simulated SAR images.....	4
2.1 FACETS electromagnetic code	4
2.2 Computer-aided design model of SLICY	6
2.3 SAR image simulation and measured data	8
3 Analysis of simulated SAR images	9
3.1 Comparison between computed SAR images and measured data.....	9
3.2 Analysis of the simulated images	13
3.3 Cavity computation	20
4 Conclusions.....	22
References	23
Annex A .. Validation of cavity computation in FACETS	25
A.1 Experimental set-up of the cylindrical duct apparatus	25
A.2 RCS measurements and computations of a duct	27
A.2.1 RCS measurements of the duct	27
A.2.2 Comparison between measured and computed data	28
A.2.3 SLICY cavity RCS computation	28
Distribution list	31

List of figures

Figure 1 Top: front view of the SLICY target [5]. Bottom: rear view of the target.	3
Figure 2 Scattering primitives: a) cylinder, b) flat plate, c) dihedral, d) top-hat (dihedral), e) trihedral, f) cavity.	5
Figure 3 CAD model of SLICY.	7
Figure 4 Identification of various scattering primitives on SLICY.	7
Figure 5 Comparison between computed and measured images at 15-degree elevation angle.	11
Figure 6 Comparison between computed and measured images at 30-degree elevation angle.	12
Figure 7 Comparison between measured and computed SAR images at 15-degree elevation angle. Source of the scattered returns are identified and labelled.	14
Figure 8 Comparison between measured and computed SAR images at 30-degree elevation angle. Source of the scattered returns are identified and labelled.	15
Figure 9 An illustration of contributions from various scattering primitives to the computed SAR images: a) visual view of SLICY as seen by the radar, b) corresponding view of the SAR image projection, c) scattering primitives on SLICY, d) to h) computed SAR images with a different scattering primitive switched off, one at a time.	p.16
Figure 10 Comparison of SAR images at edge-on aspects at 30-degree elevation angle.	18
Figure 11 Comparison of SAR images at edge-on aspects at 15-degree elevation angle.	19
Figure 12 Computation of diffraction effect: a) Edges from SLICY used in diffraction computation, b) SAR image from diffraction only, c) SAR image of SLICY, d) SAR image from diffraction only, same intensity scale as Figure 12c.	20

1 Introduction

Target identification using radar images provides an important function in surveillance applications. Radar imaging provides an effective means to collect target information for identification under all-weather conditions. It can be carried out effectively over long distances, day or night, and is capable of producing high resolution images. The actual collection of the target image data is only one of many technical challenges. One of the more challenging tasks is the processing and interpretation of the collected image data for extracting relevant target information, for example, in identifying unknown targets for threat assessment in Combat Identification and situational awareness. In order to exploit the full potential of radar images, numerical simulation techniques can help to facilitate the development of radar imaging applications. Some examples of radar imaging applications are in the areas of Non-Cooperative Target Recognition (NCTR), Automatic Target Recognition (ATR), operator-aided target classification, intelligent target selection system, aim-point refinement system for anti-ship missile seekers and multi-static radar imaging of small radar cross-section (stealth) targets. Radar images such as High Range Resolution profiles, and Synthetic Aperture Radar/ Inverse Synthetic Aperture Radar (SAR/ISAR) images are typically used as target images in these applications.

Radar target images can be simulated using computational electromagnetic (EM) codes and CAD models of the targets. Results from a previous research study [1] have indicated that many of the current synthetic target image generation tools have not yet matured enough to the point of providing high fidelity target images that can be used reliably as database in a classifier for target identification purposes. There is a common consensus that both the EM code and the CAD modeling technologies need further research and development efforts. Technical issues on the quality of the computed images using electromagnetic code and requirements on CAD modeling to support accurate high fidelity target images are investigated in this report.

Electromagnetic codes for computing radar images of complex targets such as aircraft, ships and ground vehicles have been available commercially for some time. A comprehensive study on the performance of a number of EM codes has already been conducted. Computed images from two commercial EM codes, FACETS and XPATCH, and a Dutch-developed code RAPPORT were compared with measured in-flight aircraft data in a number of detailed studies. It was found from these studies that none of these codes was able to generate aircraft images with adequate fidelity to be useful as signature database for reliable air target recognition. There is a general lack of documentation in the open literature that describes validation results of the EM codes using direct comparison between simulation and measurement for large complex targets. There are concerns regarding the lack of a well-defined methodology to achieve simulation-to-measurement validation with a consistent level of accuracy [2]. Thus there is a need to develop means to characterize EM codes in a definitive manner to provide a clear and precise assessment of their performance.

In this report, the process of validating the EM code FACETS is discussed. The EM code is validated by direct comparison with measured SAR images of a canonical target. The FACETS code is a UK-developed commercial code; it is capable of generating synthetic SAR images of complex targets such as aircraft, ships and ground vehicles. It has a modular algorithmic structure that allows it to facilitate the computational process using a combination of different scattering processes, for example, single bounce (flat-plate), double bounce (dihedral), triple bounce (trihedral), edge diffraction (cylinder and top-hat), cavity (hollow cylinder) and shadowing (obstructions between parts on the target). This modular function provides a flexible combination of computing parameters and allows the computed images to be characterized as a function of various radar scattering processes available in the code.

Measured data of high resolution SAR images of a test target composed of a collection of scattering primitives (e.g., flat-plate, cylinder, dihedral, trihedral, hollow cylinder and top-hat) are used for comparative study to validate the simulation of images. This canonical target is known as SLICY (Sandia Laboratory Implementation of Cylinders). The SLICY target is one of many targets that are compiled in the MSTAR SAR image datasets [3]. An illustration of the SLICY target is shown in Figure 1. The purpose of this target is to provide researchers a means to validate their EM code's algorithm using a well-defined target [4]:

“The ‘Slicy’ target is a precisely designed and machined engineering test target containing standard radar reflector primitive shapes such as flat plates, dihedrals, trihedrals, and top hats. The purpose of this target is to allow *Image Understanding* developers the ability to validate the functionality of their algorithm with a simple known target”

To assess and quantify the validation process of the simulated radar images, a comparative analysis framework is developed. A series of investigations to examine the computed SAR images by comparing with the measured images of the SLICY target is conducted. This provides a basis for a proper understanding on how to compute accurate SAR images of more complex targets such as aircraft, military ground vehicles and naval vessels. Some of the relevant applications that can be benefited from target image simulation are: 1) compiling databases for target classifiers (e.g., Non-Cooperative Target Recognition), 2) training human operators in assisted ISR (Intelligence, Surveillance and Reconnaissance) image analysis for maritime applications, 3) characterizing stealth target signature characteristics, 4) 3D target image visualization and 5) polarimetric radar image computation.



Figure 1 Top: front view of the SLICY target [5]. Bottom: rear view of the target.

2 Generation of simulated SAR images

2.1 FACETS electromagnetic code

The FACETS electromagnetic code was acquired, as part of the TIF (Technology Investment Fund) project on Non-Cooperative Target Recognition, to provide a capability to compute radar images of aircraft. The code was developed by Thales Defence Information Systems, UK. FACETS computes the radar cross-section and SAR image of a target using the shooting-and-bouncing ray method as the principal technique. This ray tracing method is valid for modeling scattering processes at frequency such that the object to be computed is at least 10 wavelengths in dimension or bigger. Multiple scattering on the target due to surface to surface interaction and reflection (e.g., dihedral and trihedral scattering sites) is computed by a combination of geometrical and physical optics. Edge scattering is handled using various diffraction methods, such as curved surface diffraction, reflection diffraction, edge travelling wave and surface creeping wave. Although the diffraction effect is mostly a second order effect compared to the dihedral and trihedral scattering processes, it can be important for modelling the fine details in the radar cross-section (RCS) scattering processes and it can contribute considerably to the target image under some circumstances. In the case of stealth targets, they have no dihedral and trihedral sites; hence diffraction could have a considerable contribution to a target image. FACETS can also be used to compute scattering from cavities such as aircraft intake ducts.

FACETS has the capability to compute SAR image of a target that has different surface material types: perfect electric conducting, dielectric and radar absorbing materials. FACETS can also provide a range of computation options, for example, mono-static, bi-static, near-field or far-field scattering. Furthermore, 1-dimensional HRR profiles and 2-dimensional SAR/ISAR images of the targets can be computed simultaneously in FACETS. Input parameters required are the radar centre frequency, radar bandwidth, angular aperture size and target aspect (azimuth and elevation). The computations are done for all four polarizations simultaneously (VV, HH, VH and HV), generating fully polarimetric target images.

Target geometry information required by FACETS is provided by a CAD model of the target. FACETS accepts only geometry given by the curved surface representation known as Parametric Bi-Cubic surfaces. Conventionally, curved surfaces in a CAD model are given by the NURBS (Non-Uniform Rational B-Splines) format. A NURBS surface is represented by a number of piece-wise polynomial fitting curves to provide a smooth geometrical fit to the target's shape. In order for FACETS to utilize the target information, the CAD model has to be converted from the NURBS format to the Parametric Bi-Cubic format. The CAD software tool, PATRAN is used for the format conversion.

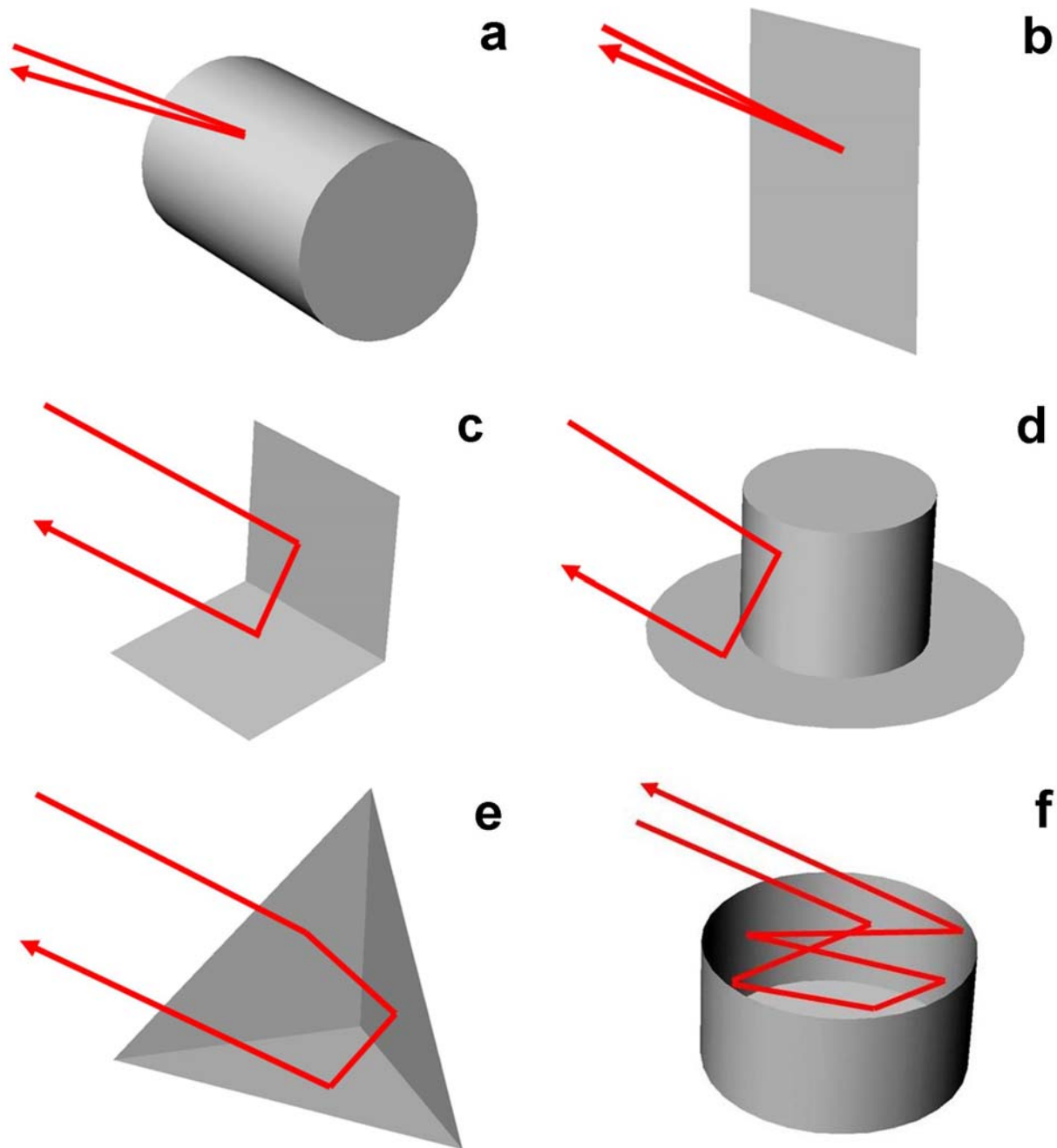


Figure 2 Scattering primitives. a) cylinder, b) flat plate, c) dihedral, d) top-hat (dihedral), e) trihedral, f) cavity.

FACETS has a modular structure for computing various scattering processes. It has a single-bounce ray-tracing algorithm that computes the basic scattering from surface types such as flat plates, cylinders and spheres. FACETS has conceded that it would be difficult to accurately account for, in an automatic manner, the more complex scattering processes such as double-bounce (dihedral), triple-bounce (trihedral), cavity (hollow structure) and diffraction from edges. Thus, FACETS requires all of these scattering processes to be specified for computation; that is, the locations of the various types of scattering primitives on the target must be identified and fed in manually. Graphical illustrations of these scattering primitives are shown in Figure 2. For real-world complex targets such as naval ships and aircraft, the nominations of all the scattering primitives could be quite labor intensive. However, for a relatively simple canonical target such as SLICY (Figure 1), this is quite manageable. It will be shown that being able to identify and account for all the appropriate scattering processes on the target is crucial to the simulation of high fidelity SAR images. It will be demonstrated in the following analysis that the human-assisted algorithmic structure in FACETS offers some useful and insightful glimpses of what some of the requirements and challenges are for generating high fidelity simulated SAR images.

2.2 Computer-aided design model of SLICY

SLICY is a vehicle size test target that features a number of scattering primitives. The purpose of this target is to allow electromagnetic code developers a better understanding of the scattering processes and the ability to validate the functionality of their algorithms against a simple known target. Figure 3 shows a CAD drawing of SLICY. The dimensions of SLICY are 2.75 m in length, 2.445 m in width, and the height of the rectangular box is 0.765 m. The tall cylinder with a close-top is 0.915 m in height with a 0.66 m diameter; the short hollow (open-top) cylinder is 0.458 m in height and a 0.66 m diameter. The inner wall of the hollow cylinder behaves like a cavity, a special type of scattering primitive. There are also a small trihedral corner reflector, a quarter cylinder and two step-like trihedral corners on SLICY. The scattering primitives on SLICY are identified in Figure 4.

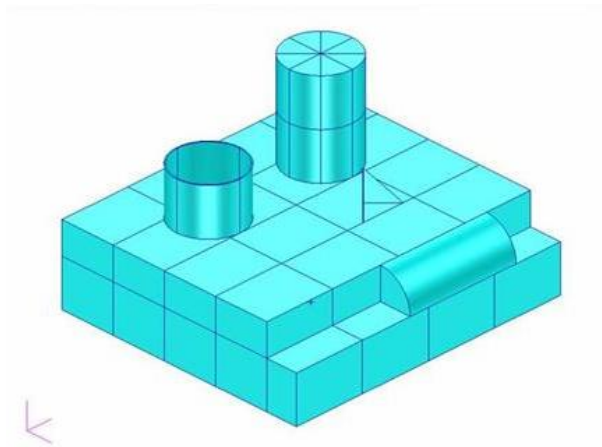


Figure 3 CAD model of SLICY.

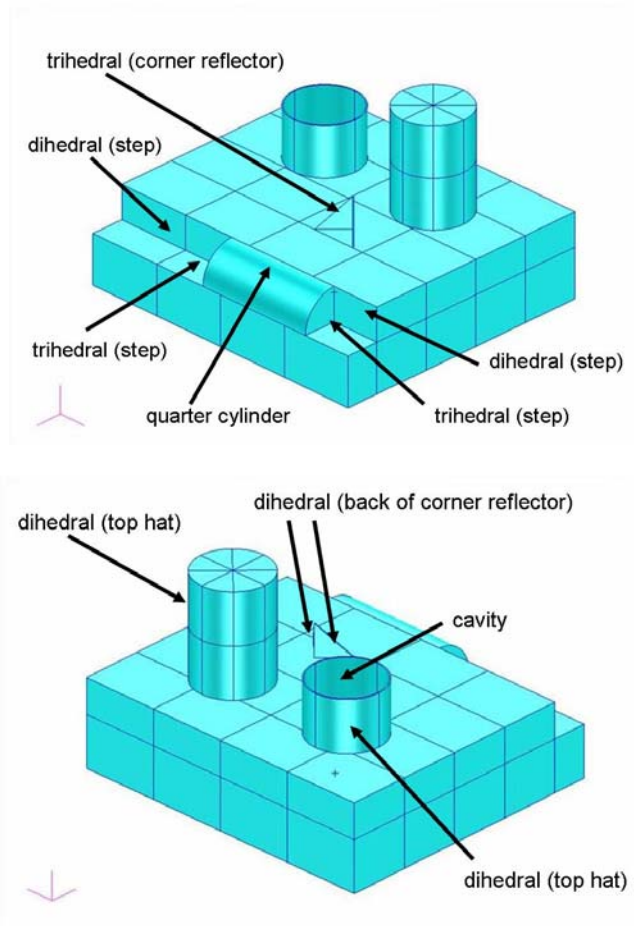


Figure 4 Identification of various scattering primitives on SLICY.

2.3 SAR image simulation and measured data

To validate the FACETS computations, SAR images of SLICY are computed at two elevation look angles, 15 degrees and 30 degrees, and a full 360-degree coverage in the azimuth direction at X-band radar frequency (9.6 GHz). The generated images are then compared with the measured images of SLICY for validation.

The measured SAR images were collected using the Spotlight SAR mode; the target was stationary. Data were captured at a number of depression angles. The Spotlight SAR radar was flown several times around the target, providing multiple 360-degree azimuth coverage in the measurements. The SAR images of SLICY were cropped from larger scenes of the captured SAR data. The size of the SLICY target image is 54 by 54 pixels. The measured images have down-range and cross-range resolutions of 0.254 m based on a radar bandwidth of 591 MHz and the assumption of equal down-range and cross-range resolution [3]. The image data are, however, over-sampled to give effective down-range and cross-range pixel spacing of 0.2 m.

For comparative purposes, provision is made so that the 0.2 m pixel spacing is also incorporated in the computed image. This is achieved by using a radar bandwidth of 750 MHz and an angular aperture of 4.38 degrees. Thus the computed SAR images have a slightly better spatial resolution. This sharper resolution helps to facilitate a simpler task in the analysis by making it easier to identify various scattering centres on the computed images of SLICY.

The SLICY target is computed as an isolated object; that is, there is no ground-plane interaction included in the computation. FACETS computes the single-bounce process for the whole target by default automatically. In addition, locations of the dihedrals, trihedrals, cavity, and edge diffraction are identified manually on the CAD model. A composite SAR image of the target is then generated from a combination of these scattering processes.

3 Analysis of simulated SAR images

3.1 Comparison between computed SAR images and measured data

Figures 5 and 6 show the comparative results between the computed SAR images from FACETS and the measured images from the MSTAR datasets at 15-degree and 30-degree elevation angles respectively. The images are sampled at a 45-degree interval over a full 360-degree azimuth coverage (at 0, 45, 90, 135, 180, 225, 270, 315 degrees). It can be seen from Figures 5 and 6 that the comparison between the computed and measured images produces very good agreement visually for all azimuth angles and at both elevation angles.

Visual inspection of Figures 5 and 6 reveals that all the major scattering sites that are present in the measured images are also present in the computed images. These observations provide a direct validation of the SAR image simulation process by FACETS. There have been recent efforts in an attempt to validate other electromagnetic codes using the SLICY target as benchmark [6][7]. However, validation by direct comparison between the measured and computed images of a target has not yet been reported in the literature. The successful validation results obtained here can be summarized as a consequence of two very basic requirements: 1) a CAD model that is accurate in representing the types of scattering primitives and their locations on the target, 2) a numerical electromagnetic code that can correctly and reliably compute these scattering primitives as single-bounce, double-bounce, triple-bounce or cavity.

Although these two requirements may seem to be obvious and trivial, it is not easy to confirm whether these have actually been met in practice, especially for a complex target. In the case of the SLICY target, a proper and accurate CAD model describing the various scattering primitives and their locations on the target is possible. This may be rather an exception because well-defined scattering primitives are involved and there are only a small number of these on SLICY. The geometrical location of a scattering primitive should be within the required resolution of the SAR image. Thus, the higher the image resolution, the smaller the allowable tolerance on the error of the location of a particular scattering primitive on the target. Furthermore, the type of scattering primitive must be accurately described so that single-bounce, double-bounce, triple-bounce and multi-bounce (i.e., cavity) can be assigned properly either by an algorithm within an EM code, or by a human operator as in the case of FACETS. It can be seen that if a location in the CAD model where a double-bounce site is misinterpreted as triple-bounce, or vice versa, the computed SAR images will not be consistent and accurate over a range of azimuth and elevation angles when they are compared with measured SAR images. If a double-bounce/triple-bounce site is misinterpreted as single-bounce, a peak could be missing from the computed image. The most difficult case is that of computing a cavity. Depending on the diameter and length of the cavity, the number of bounces varies.

FACETS does an admirable job in coping with this problem. One can assign a maximum number of bounces in a cavity to get a fairly accurate output; but that is obtained at a cost of computational time. However, when one assigns a smaller number of bounces to save computing time, the output may not be accurate.

For real-world complex targets such as aircraft, ships and battle tanks, the geometrical shapes of the targets may not be well-defined scattering primitives, and the problem of what is “proper and accurate” is not straight-forward. A double-bounce or a triple-bounce may not be localized to within tens of wavelengths from an obvious dihedral-like or trihedral-like site. It could be meters (on an aircraft) or tens of meters (on a large ship) apart where scattering surfaces happen to form dihedral-like or trihedral-like surfaces. The problem of CAD model fidelity had prompted an exploratory study. Realizing that there was no satisfactory systematic approach that can be devised to address the fidelity issue of a CAD model for a complex target, a large-scale exploratory approach was taken. Highly precise CAD models of 2 aircraft were created using laser-scanning techniques on the actual aircraft. Computations using these CAD models were to be compared with measured SAR data collected from the actual aircraft. This was intended as a first step to try to understand what are needed as requirements for producing high fidelity CAD models. Results from this study have not yet been published.

It is also not a straightforward task to ensure that all the relevant scattering sites are represented properly and accounted for in the CAD model. This is due to the fact that the shapes of real targets are much more complex and more difficult to build properly. In addition, different versions of the same target could also have notable difference in some places on the target. For example, a jet fighter can carry different store and weapon configurations; this could alter the scattering returns from the target considerably.

Furthermore, there are also questions whether a high frequency, ray-tracing EM code can identify and compute reliably the various scattering primitives correctly as single-bounce, double-bounce, triple bounce or cavity. The FACETS code has addressed and resolved these issues by manual input of appropriate information for computation; it relies heavily on the experience and judgment of the human operator to provide correct identification of the scattering primitives.

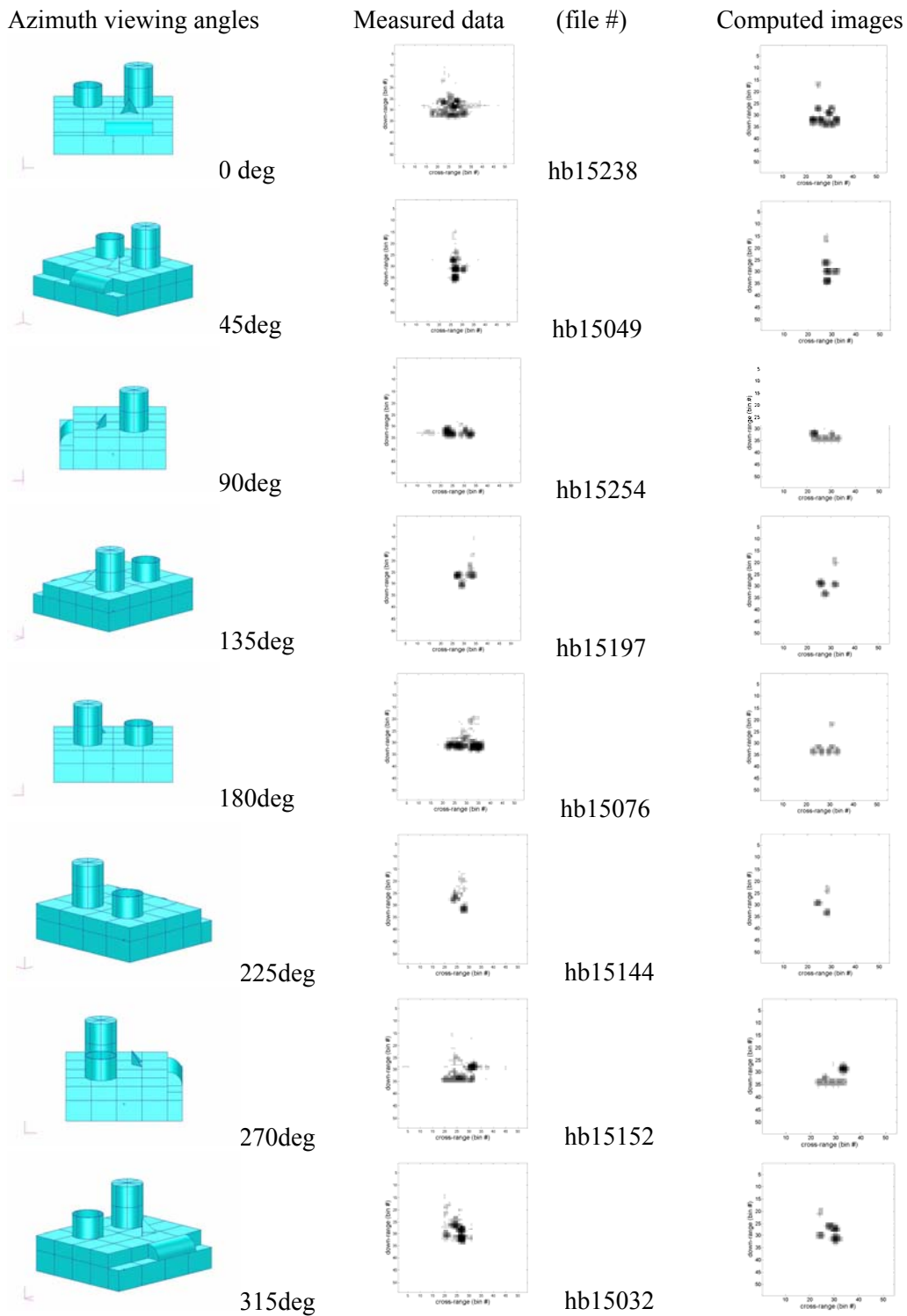


Figure 5 Comparison between computed and measured images at 15-degree elevation angle.

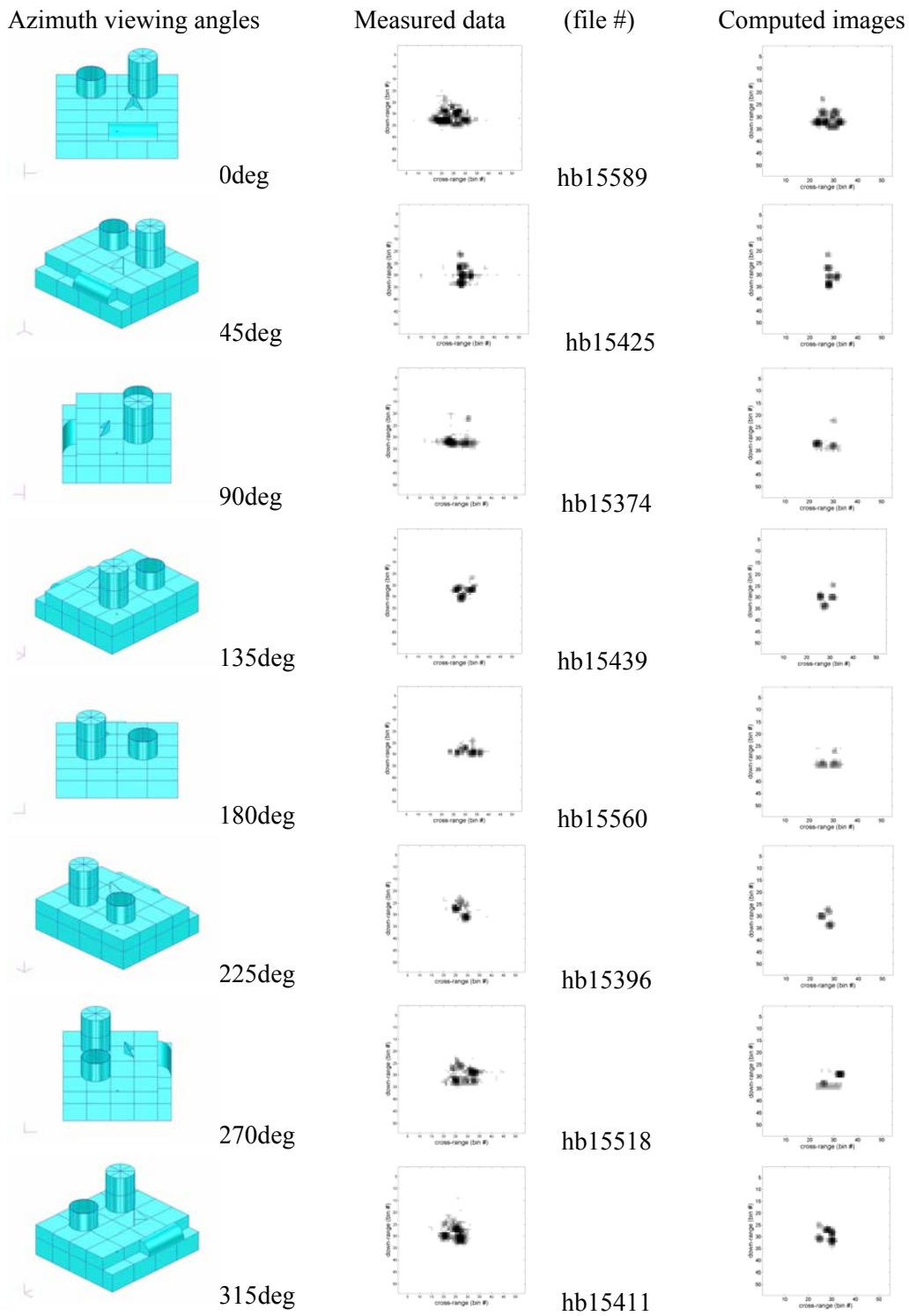


Figure 6 Comparison between computed and measured images at 30-degree elevation angle.

3.2 Analysis of the simulated images

The use of the SLICY target provides useful insights into the computational process of synthetic image generation. Figures 7 and 8 show some of the better matches between the computed and the measured SAR images at 15-degree and 30-degree elevation angles respectively. The scattering primitives responsible for the scattered returns are labelled in the computed images. Since FACETS has a modular structure in the computation of various scattering processes, the contribution of each individual scattering primitive to the SAR image can be confirmed by having it disabled in the computation. To illustrate, Figure 9 shows a sequence of computed SAR images of SLICY at 315-degree azimuth angle, with each of the five scattering primitives disabled, one at a time, in the computations. Figure 9c is the computed SAR image with all the scattering primitives on SLICY; it serves as the reference image. By disabling each scattering primitive in the image computation, the sequence of images (Figures 9d to 9h) provides a clear illustration of the scattering primitives that are responsible for composing the SAR image.

It is noted from Figures 7 and 8 that the better matches between the computed and measured images are from viewing angles in which SLICY is at a 45-degree viewing angle with respect to the straight edges on the base of the target. That is, the corners of SLICY are pointing towards the radar; these viewing angles correspond to 45, 135, 225 and 315 degrees in azimuth. These target orientations essentially minimize the scattering returns from the flat surfaces on the sides of the rectangular base of SLICY. Thus the scattering returns that are seen in the SAR images are mainly coming from the dihedrals and trihedrals and the hollow cylinder (cavity) as indicated in Figure 9.

The comparison between the measured and computed SAR images with SLICY positioned at edge-on aspect with respect to the radar (e.g., azimuth angles at 0, 90, 180, 270 degrees) are shown in Figures 10 and 11 for elevation angles of 30-degrees and 15-degrees respectively. These comparisons are more complex; the agreements, although still quite good, are not as clean cut and as definitive as those in Figures 7 and 8. All the scattered returns from the scattering primitives are seen in both the measured and computed images. The identities of these scattered returns have been verified by the procedure of disabling each of the scattering primitives, one by one as described above. However, there are spurious returns in the measured images that are not present in the corresponding computed images at these edge-on azimuth angles.

Measured data (file #, viewing angle)

Computed images

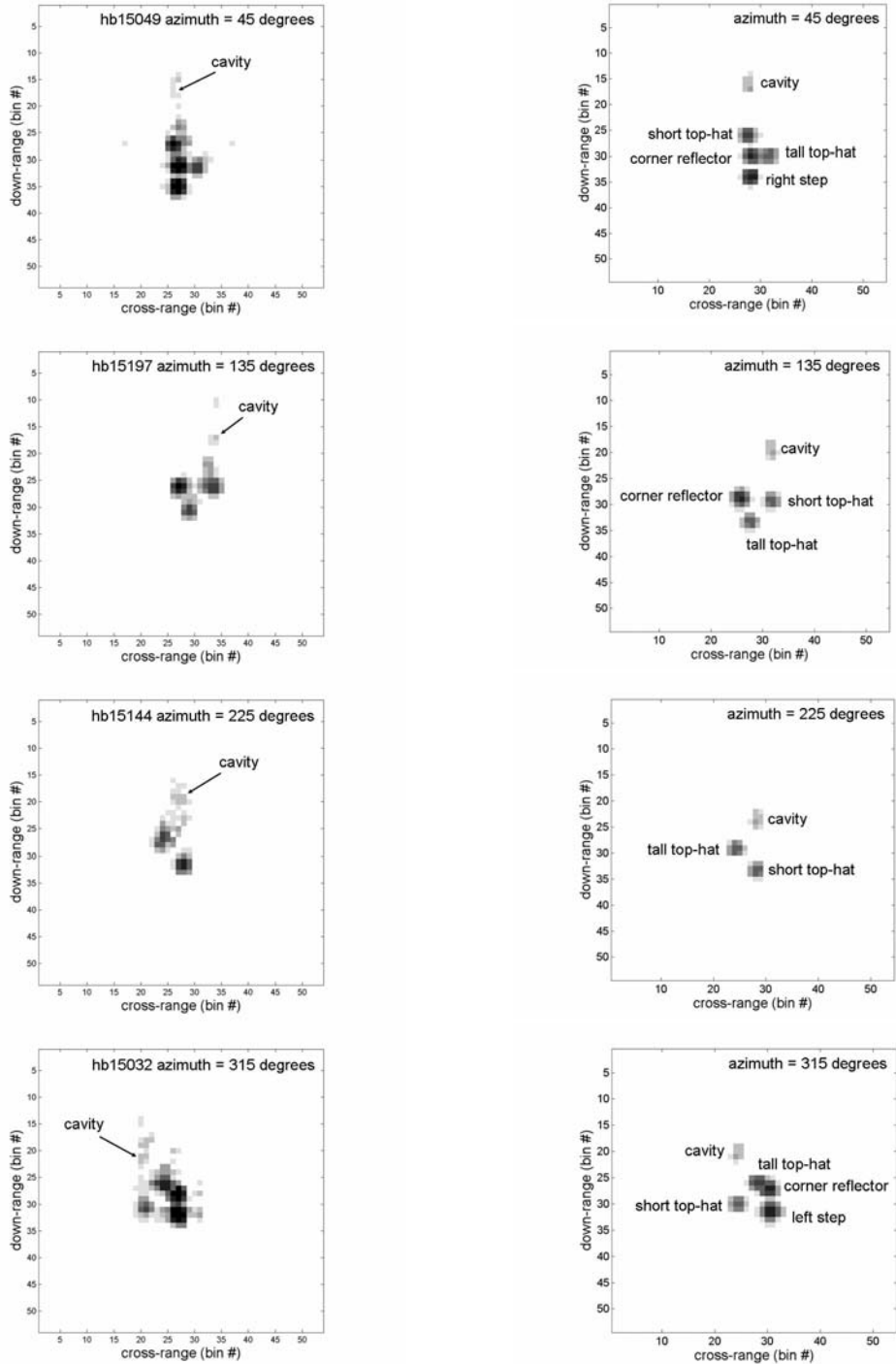


Figure 7 Comparison between measured and computed SAR images at 15-degree elevation angle. Source of the scattered returns are identified and labelled.

Measured data (file #, viewing angle)

Computed images

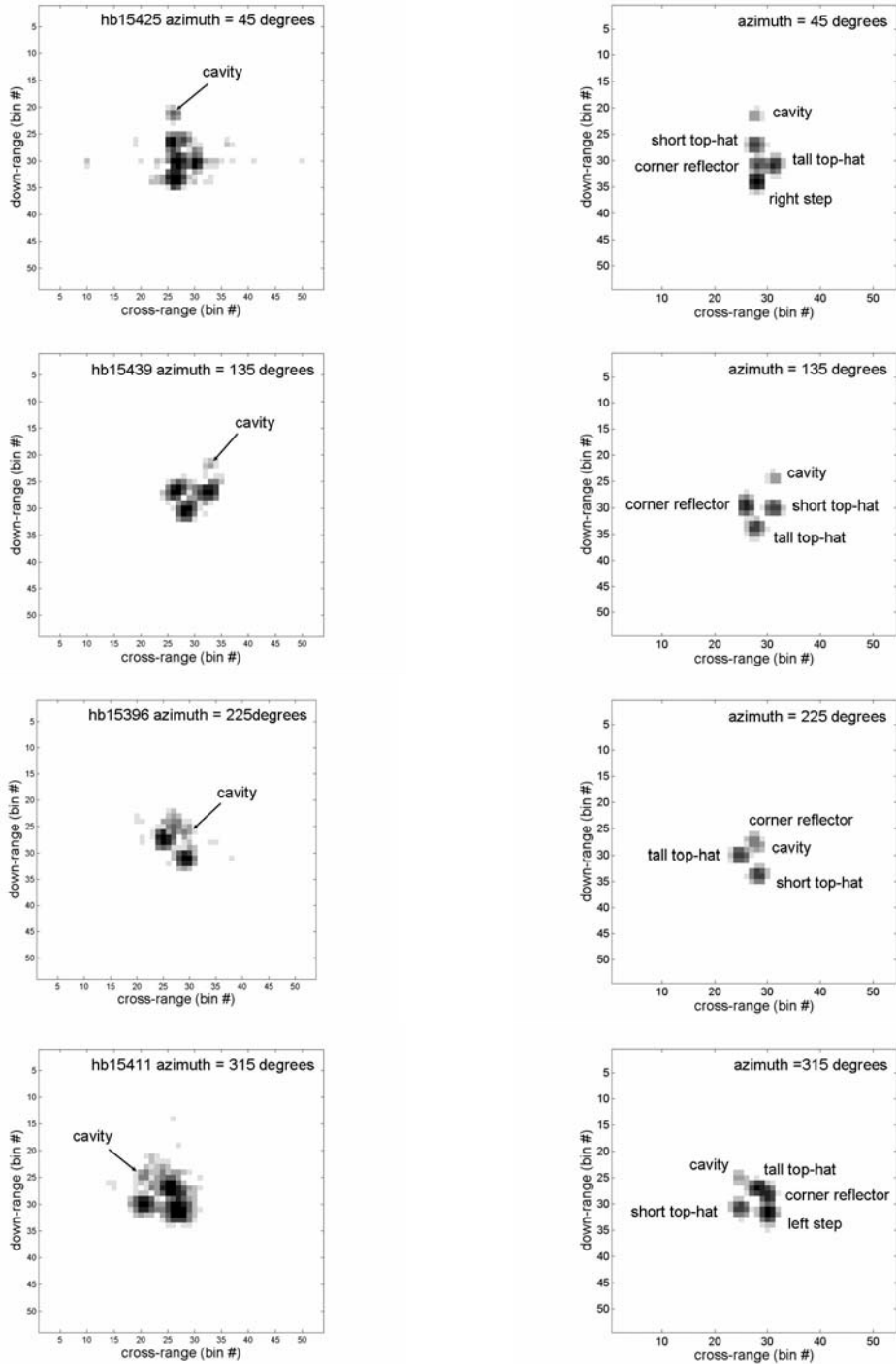
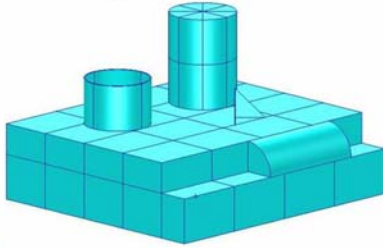
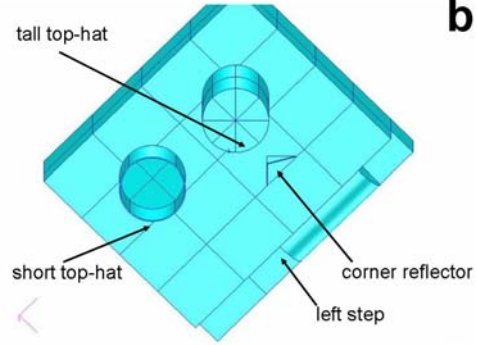


Figure 8 Comparison between measured and computed SAR images at 30-degree elevation angle. Source of the scattered returns are identified and labelled.

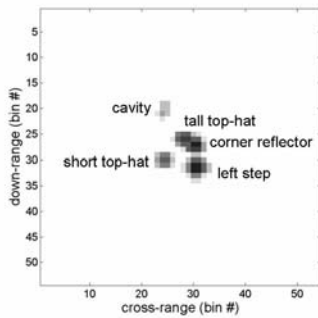
elevation = 15 degrees
azimuth = 315 degrees



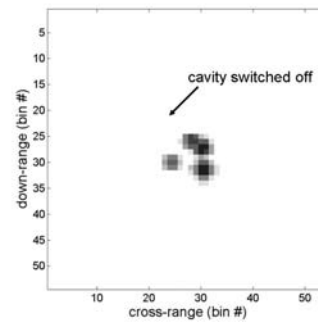
a



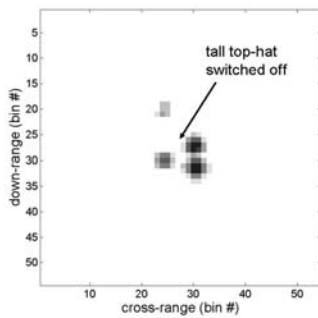
b



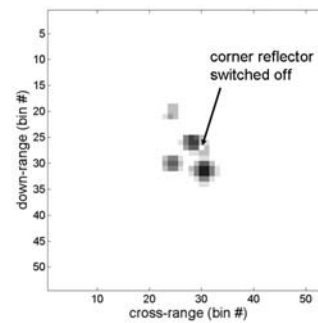
c



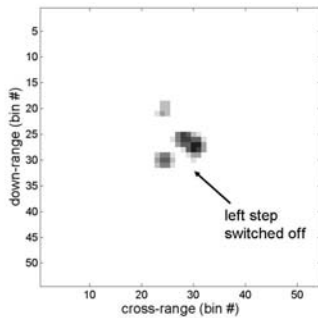
d



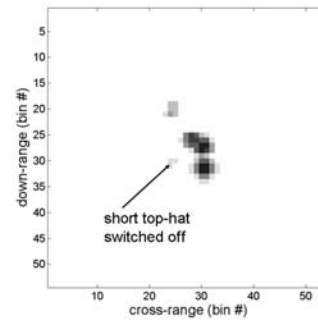
e



f



g



h

Figure 9 An illustration of contributions from various scattering primitives to the computed SAR images. a) visual view of SLICY as seen by the radar, b) corresponding view of the SAR image projection, c) scattering primitives on SLICY, d) to h) computed SAR images with a different scattering primitive switched off, one at a time.

In the 30-degree elevation case (Figure 10), scattered returns from the rectangular base of SLICY are detected in the measured images, although not very strongly. The scattered returns from the base in the computed images are considerably weaker than those in the measured images. This could be due to the fact that there is no ground-target interaction included in the computed images. Whereas, in the case of the measured images, it is reasonable to assume that there may be a dihedral formed between the ground (dielectric) and the sides of the rectangular base, providing some scattered signals.

Besides the more noticeable scattered returns from the sides of the base, the measured images at these edge-on azimuth angles also pick up spurious scattering returns from the target. These are indicated by the “?” symbol on the measured images in Figure 10. They occur along the straight edges and at the corner edges of the rectangular base of SLICY as localized point-like spots. These extraneous scattered returns have no obvious corresponding identifiable scattering sites on the target. However, it is generally accepted and expected that there could be imperfections in the real measured data, causing various anomalous effects. A notable point that can be made is that the spurious returns seem to occur exclusively at the edge-on azimuth viewing angles. These may be caused by diffraction effect from the straight edges and the corner edges.

Since FACETS has the capability to compute edge diffraction effect, this is investigated. The edges on SLICY are identified for diffraction computation; this is shown by the dashed lines in Figure 12a. Initially, only diffraction is computed; that is, computations from single-bounce, double-bounce, triple-bounce and cavity are switched off. The SAR image of SLICY due to diffraction effect only is shown in Figure 12b; it is seen that only the two long edges running across the image are visible in the SAR image. Figure 12c shows the SAR image of SLICY when diffraction, single-bounce, double-bounce, triple-bounce and cavity are all computed. To get an idea of the contribution to the SAR image due to diffraction, the pixel intensity of Figure 12b is rescaled to match the pixel intensity shown in Figure 12c. The SAR image due to diffraction only with rescaled pixel intensity is shown in Figure 12d. It can be seen that the contribution due to diffraction is negligible to the overall image, by comparing Figure 12c and Figure 12d. The contribution from diffraction is about 30dB lower in intensity. This is not surprising since diffraction is expected to be a second order effect.

In the 15-degree elevation images as shown in Figure 11, scattering returns from the sides of the rectangular base are much more pronounced in the measured images. They also appear in the computed images. Since the computations are done without any ground-target interaction included, the more noticeable returns from the sides of the base in the computed images could be attributed to the smaller elevation angle in the target aspect, making the scattering closer to the specular reflection condition than that in the 30-degree elevation case. There appears to be less spurious scattering returns observed in the measured images at 15-degree elevation. The measured and computed images appear to

Measured data (file #, viewing angle)

Computed images

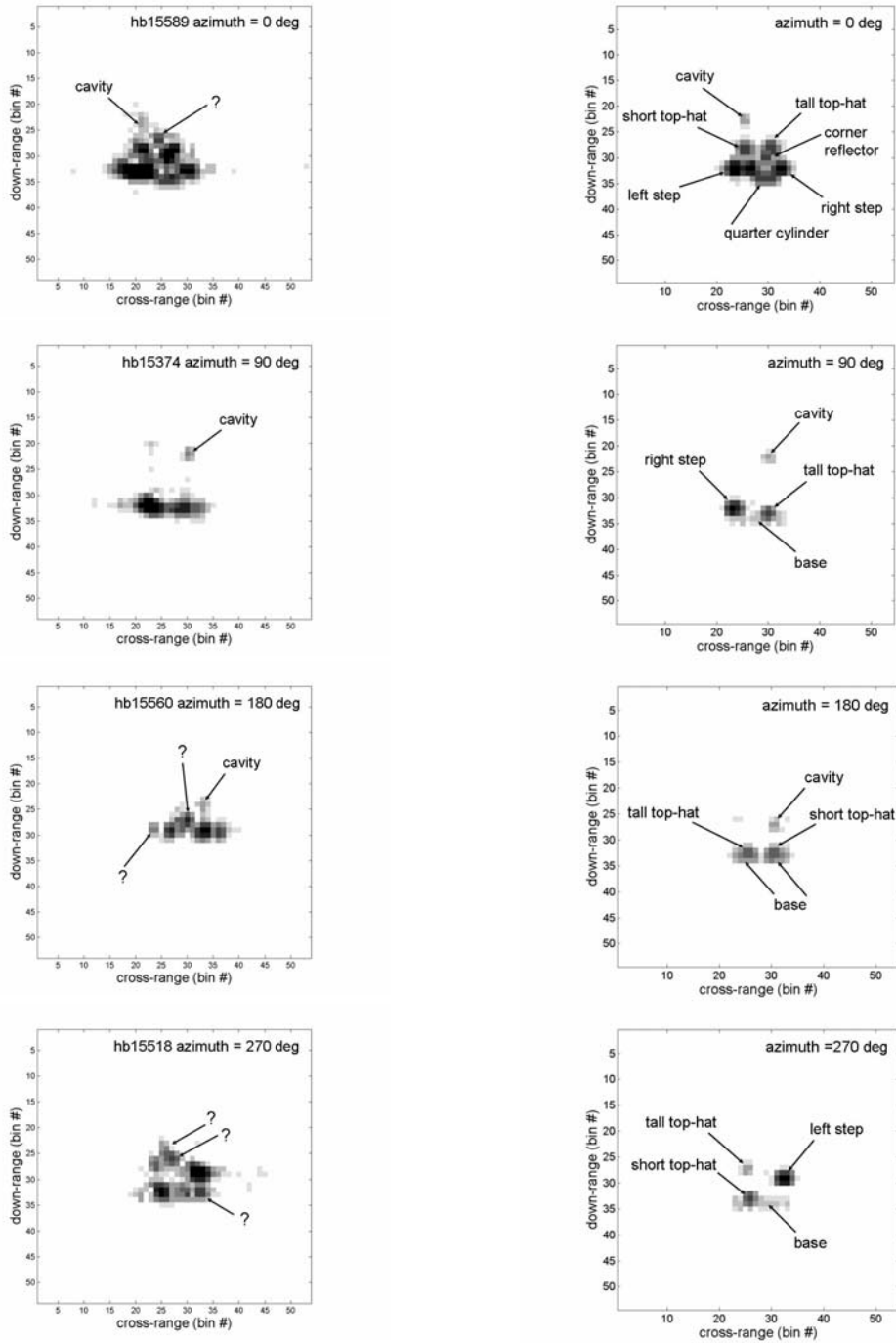


Figure 10 Comparison of SAR images at edge-on aspects at 30-degree elevation angle.

Measured data (file #, viewing angle)

Computed images

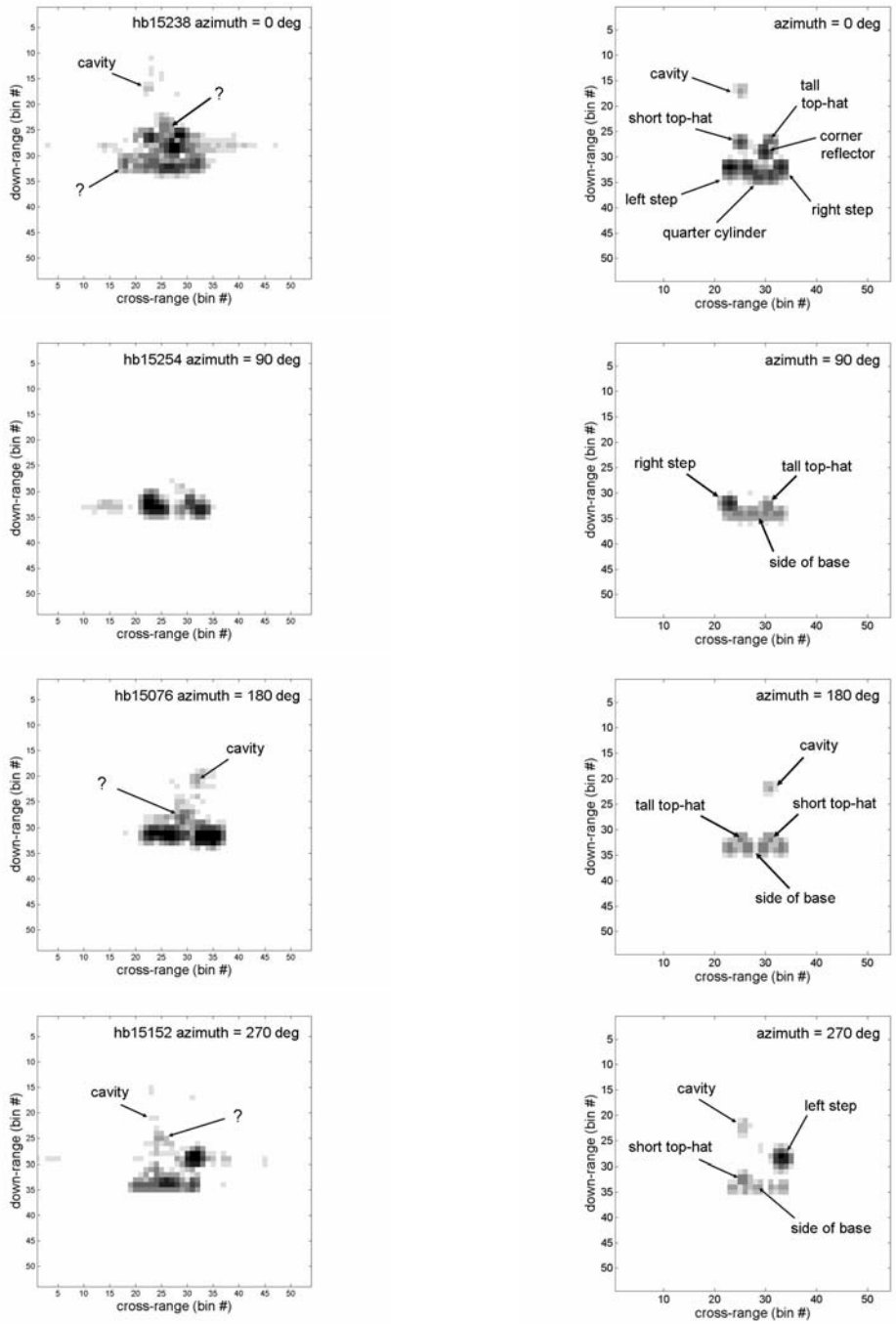


Figure 11 Comparison of SAR images at edge-on aspects at 15-degree elevation angle.

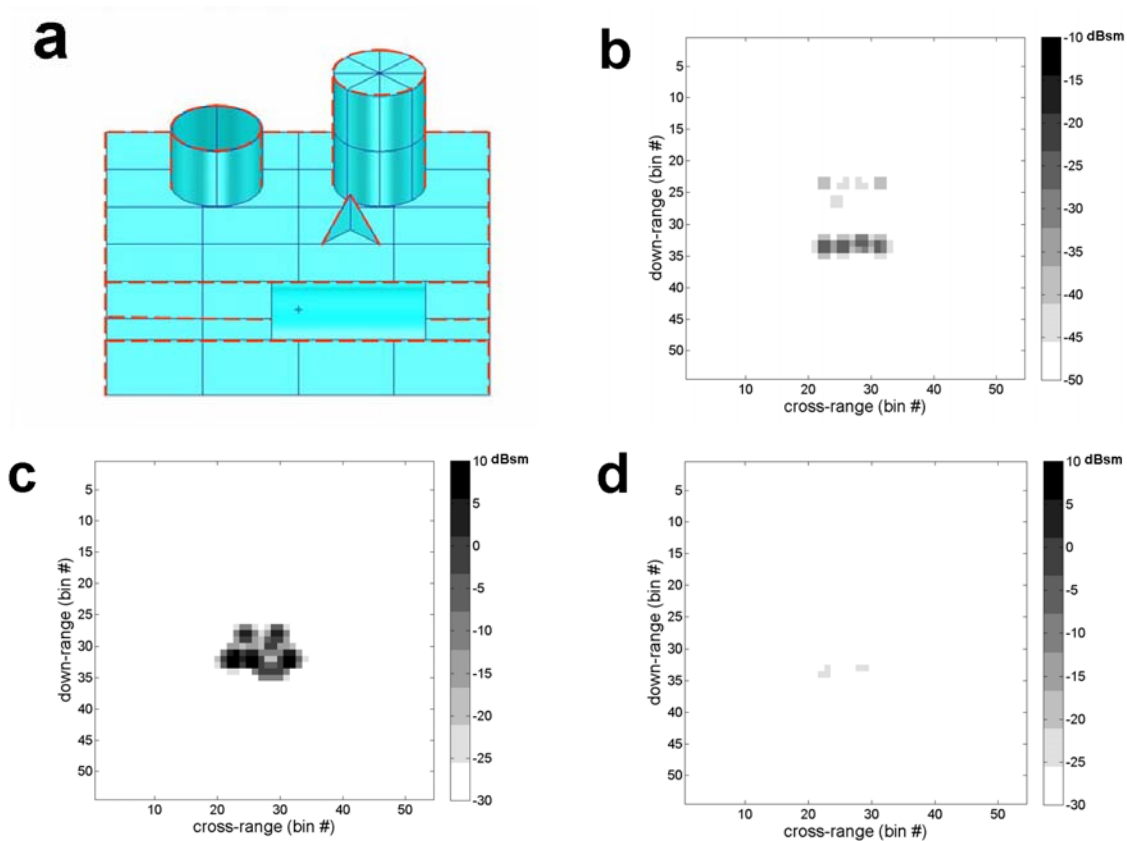


Figure 12 Computation of diffraction effect: a) Edges from SLICY used in diffraction computation, b) SAR image from diffraction only, c) SAR image of SLICY, d) SAR image from diffraction only, same intensity scale as Figure 12c.

be in better agreement than those at 30-degree elevation. This is clearly seen by comparing the computed images against the measured images between Figures 10 and 11.

3.3 Cavity computation

A notable success of the computed images is the prediction of the scattered returns from the cavity of the short hollow cylinder. The “faint smudge” from the cavity return can be clearly seen in Figures 7, 8, 10 and 11, in both the measured and computed SAR images. The cavity return is indicated on these figures. The cavity return appears at a location on the SAR image that does not correspond physically to where the hollow cylinder is located. This is because the cavity scattering is made up of many bounces along the inner wall of the hollow cylinder due to the large incidence angles of the incident radar rays with respect to the vertical axis of the cylinder. Since the down-range axis of the SAR image corresponds to the differential time delay of the radar rays traveling to-and-fro the radar, the multiple bounces create a longer time delay and hence a displaced spot for the cavity on the SAR image. The relative location of the cavity return with respect to the

short cylinder is in excellent agreement between the measured and computed images for all azimuth viewing angles; this can be seen in Figures 7, 8, 10 and 11. Furthermore, results from cavity computations have been validated by measured data. Scattered radar cross-section returns from cylindrical cavities as a function of incidence angles are found to be in excellent agreement with experiments. The details of the comparison are given in Annex A.

4 Conclusions

Simulation-to-measurement validation of the electromagnetic code FACETS by employing the canonical target SLICY, with well-defined scattering primitives is presented. It is shown that a consistent level of accuracy has been achieved in the computed SAR images by comparing against those from measured data over 360-degree azimuth coverage at two elevation angles. It has been demonstrated that the basic scattering processes that are responsible for the scattered returns seen in the measured images can be accurately simulated. By exploiting the modular structure of FACETS, it is shown that the functionality of the image generation algorithm in FACETS can be validated, verifying its capability in handling the scattering primitives appropriately and computing them correctly.

The SLICY target was originally conceived and built with the intention of using it to help the computational electromagnetic modelling community to assess its modelling tool development. An ‘objective’ statement was provided along with the measured SAR data of SLICY: “The purpose of this target is to allow *Image Understanding* developers the ability to validate the functionality of their algorithm with a simple known target”. This work has accomplished this stated objective by demonstrating simulation-to-measurement validation through direct SAR image comparisons.

References

- [1] S. Wong, “A summary of the TIF project on Synthetic Target Signature Generation for Non-Cooperative Target Recognition”, (DRDC Ottawa TN 2005-172) Defence R&D Canada – Ottawa. Internal Publication
- [2] A. Drozd, “Progress on the development of standards and recommended practices for CEM computer modeling and code validation”, 2003 IEEE International Symposium on Electro-Magnetic Compatibility, vol.1, pp.313-316 2003.
- [3] MSTAR SAR public release datasets, 1997. <http://cis.jhu.edu/data.sets/MSTAR/>
- [4] <https://www.sdms.afrl.af.mil/datasets/mstar/targets.php>
- [5] R. Wu, J. Li, Z. Bi and P. Stoica, “SAR Image Formation via Semiparametric Spectral Estimation”, IEEE Transactions on Aerospace and Electronic Systems, vol.35, no.4, pp.1318-1333, October 1999.
- [6] W. Coburn, C. Kenyon and C. Le, “Preliminary benchmarking of radar signature prediction codes”, Proceedings of the Users Group Conference, pp.262-269, 2005.
- [7] A. M. Raynal, R. Bhalla, H. Ling and V. J. Velton, “An algorithm for target validation using 3-D scattering features”, Proceedings of SPIE, vol.6568, pp-1-8, May 2007.

This page intentionally left blank

Annex A Validation of cavity computation in FACETS

A comparative evaluation of the cavity radar cross-section data from a cylindrical duct apparatus is conducted. Cavity computations from the FACETS electromagnetic (EM) code that has a dedicated function for computing cavity RCS returns are compared with experimental data. This comparative study serves as a validation of the FACETS EM code's capability in predicting the RCS returns from a cavity structure.

A.1 Experimental set-up of the cylindrical duct apparatus

A metallic cylindrical duct made out of galvanized sheet metal with a 0.7-m diameter is constructed as the test cavity. The length of the duct can be varied from 1 m to 1.9 m by moving a terminating plate along the length of the cylinder. A CAD model drawing of the duct cavity is shown in Figure A1.



Figure A1 CAD model of the cylindrical cavity with a terminating plate at the back.

The cylindrical duct is mounted horizontally on a rotating platform. It is illuminated by the radar along the horizontal direction. A computer controlled stepping motor is used to drive the rotating platform. The rate of rotation can be varied but is nominally set at 1 degree/s for the RCS measurements. The rotational rate is consistent to within 2 seconds in a 180-second duration over many trial runs. With the stepping motor controlled by the computer, the position of the rotating platform can be reset to the original position quite accurately. Any positional error in the re-setting of the turntable comes from the backlash of the gearing system. However, the backlash error is very small and it takes many runs before a 1 to 2-degree re-setting error is noticed. RCS measurements of the duct are collected at an X-band radar frequency of 8.9 GHz; the radar operates in a pulsed mode at a radar pulse repetition rate (PRF) of 1 kHz. The received radar signals have a HH (transmit/receive) polarization.

To ensure that the backscattered radar signal collected is from inside the duct only, the exterior of the duct is covered with radar absorbing material (RAM). A photo of the duct apparatus is shown in Figure A2. The RAM tiles are effective in the 8 to 10 GHz frequency region. A background check is conducted to verify that no spurious radar return is detected from the exterior of the duct apparatus. This is done by covering the duct entrance with RAM tiles and a RCS measurement is made by rotating the duct from -60 to $+60$ degrees in the horizontal direction. The background RCS measurement is shown in Figure A3. It can be seen that the background radar return is fairly constant over the 120-degree scanned angles, indicating that there are no spurious reflections from the exterior of the duct apparatus.



Figure A2 Cylindrical-cavity experimental apparatus.

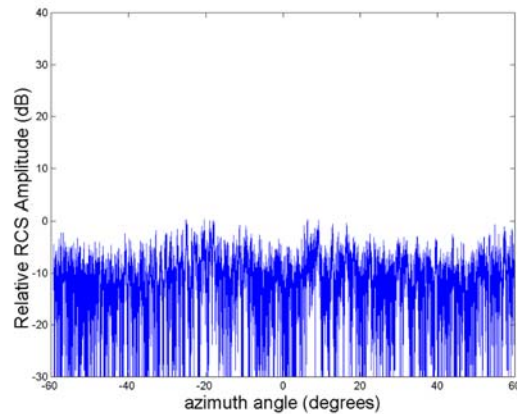


Figure A3 Background RCS measurement of the cylindrical duct.

A.2 RCS measurements and computations of a duct

A.2.1 RCS measurements of the duct

RCS measurements of the engine duct are made by scanning from -60 to $+60$ degrees along to horizontal direction (i.e., incidence angles). In the first set of measurements, the terminating flat plate (see figure A1) is placed 1 m from the duct entrance, making the cavity 1-m deep. Figure A4 (solid curve) shows the measured RCS of the engine duct as a function of incidence angle. The flat plate is then moved back to 1.9 m from the duct's entrance and another RCS measurement is made. The measured RCS scan is shown in Figure A5 (solid curve). Note that the measured RCS scans are quite symmetrical with respect to the zero-degree incidence angle. The signal-to-noise ratio of the measured RCS signal is also quite good. The signal is 10 to 30 dB above the noise floor as shown in Figure A3.

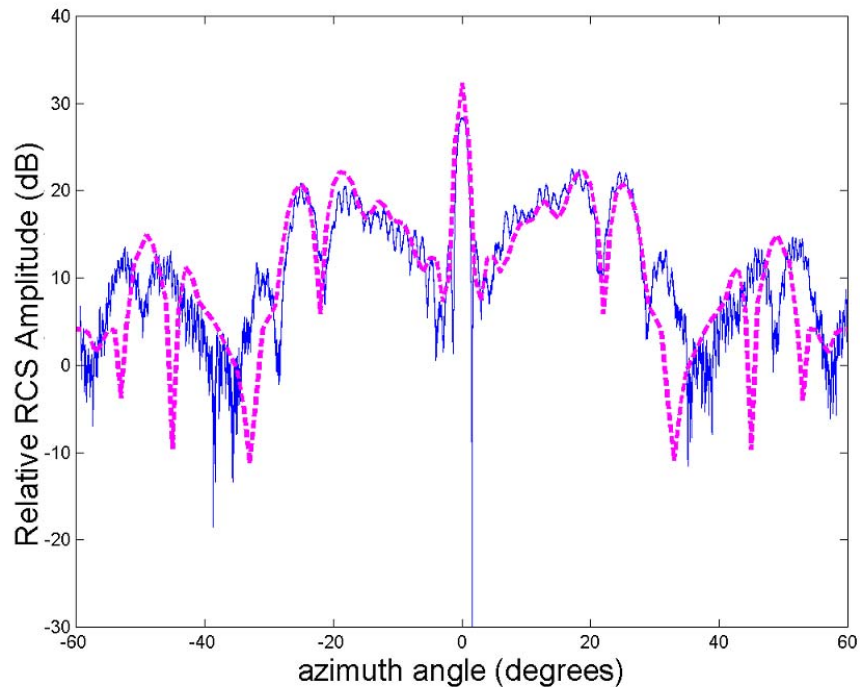


Figure A4 RCS as a function of incidence (azimuth) angle for a 1 m long cylindrical duct. Solid curve (measured); dashed curve (computed).

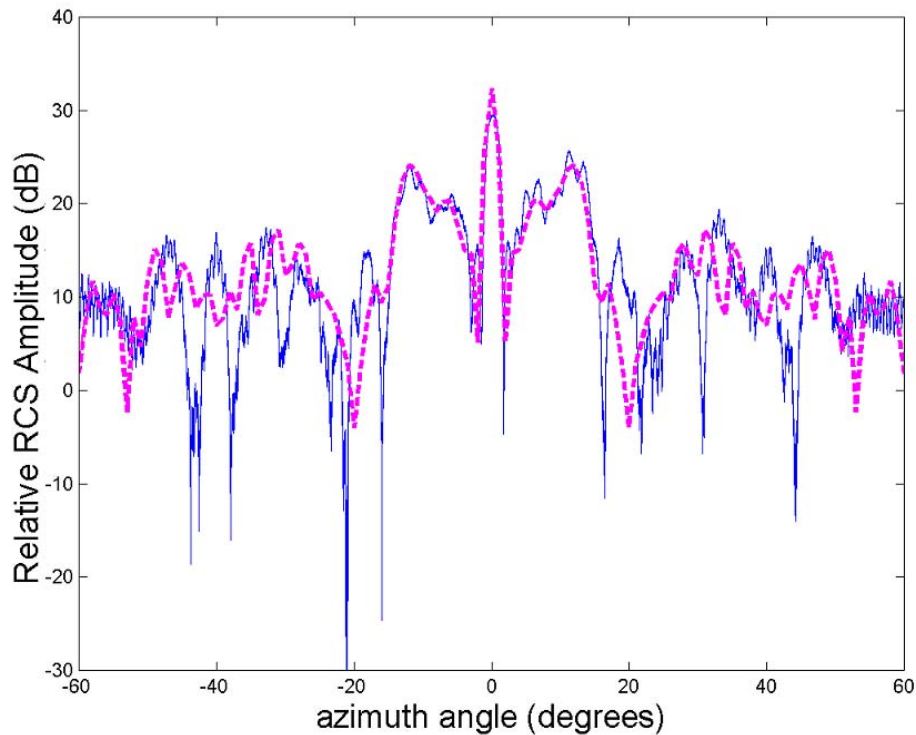


Figure A5 RCS as a function of incidence (azimuth) angle for a 1.9 m long cylindrical duct. Solid curve (measured); dashed curve (computed).

A.2.2 Comparison between measured and computed data

The dashed curves in Figures A4 and A5 show the computed RCS of the duct as a function of incidence angle from FACETS for duct lengths of 1 m and 1.9 m respectively. It can be seen that the computed RCS patterns compare very well with the measured data up to the first couple of major side lobes on both the positive and negative sides with respect to the zero-degree incidence angle. As the incidence angle becomes more oblique, the agreement of the RCS between the measured and computed results has deteriorated somewhat; but the overall agreement is still fair. Thus these comparative results indicate that the computed cavity RCS returns by FACETS are quite accurate at incidence angles near boresight.

A.2.3 SLICY cavity RCS computation

In the SLICY case, the hollow cylinder is much shorter, with a length of 0.458 m. The computed RCS values of the short cavity computed by FACETS are shown in Figure A6. The incidence angles of 60 degrees and 75 degrees correspond to the 30-degree and 15-degree elevation cases

respectively. It can be seen that at these 2 elevation angles, the RCS returns are fairly low. This accounts for the “faint” spot corresponding to the cavity return in SLICY’s SAR images.

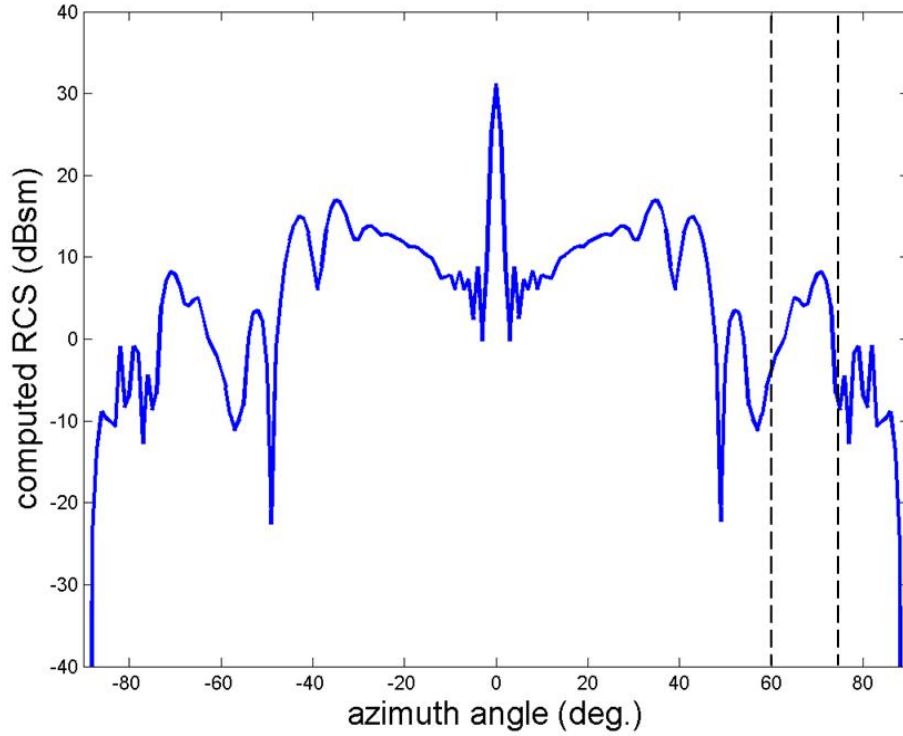


Figure A6 RCS as a function of incidence (azimuth) angle for the short hollow cylinder on SLICY.

This page intentionally left blank.

DOCUMENT CONTROL DATA

(Security classification of title, body of abstract and indexing annotation must be entered when the overall document is classified)

1. ORIGINATOR (The name and address of the organization preparing the document. Organizations for whom the document was prepared, e.g. Centre sponsoring a contractor's report, or tasking agency, are entered in section 8.) Defence R&D Canada – Ottawa 3701 Carling Avenue Ottawa, Ontario K1A 0Z4		2. SECURITY CLASSIFICATION (Overall security classification of the document including special warning terms if applicable.) UNCLASSIFIED	
3. TITLE (The complete document title as indicated on the title page. Its classification should be indicated by the appropriate abbreviation (S, C or U) in parentheses after the title.) Validation of the electromagnetic code FACETS for numerical simulation of radar target images			
4. AUTHORS (last name, followed by initials – ranks, titles, etc. not to be used) S. Wong			
5. DATE OF PUBLICATION (Month and year of publication of document.) December 2009	6a. NO. OF PAGES (Total containing information, including Annexes, Appendices, etc.) 42	6b. NO. OF REFS (Total cited in document.) 7	
7. DESCRIPTIVE NOTES (The category of the document, e.g. technical report, technical note or memorandum. If appropriate, enter the type of report, e.g. interim, progress, summary, annual or final. Give the inclusive dates when a specific reporting period is covered.) Technical Memorandum			
8. SPONSORING ACTIVITY (The name of the department project office or laboratory sponsoring the research and development – include address.) Defence R&D Canada – Ottawa 3701 Carling Avenue Ottawa, Ontario K1A 0Z4			
9a. PROJECT OR GRANT NO. (If appropriate, the applicable research and development project or grant number under which the document was written. Please specify whether project or grant.) 15e105		9b. CONTRACT NO. (If appropriate, the applicable number under which the document was written.)	
10a. ORIGINATOR'S DOCUMENT NUMBER (The official document number by which the document is identified by the originating activity. This number must be unique to this document.) DRDC Ottawa TM 2009-275		10b. OTHER DOCUMENT NO(s). (Any other numbers which may be assigned this document either by the originator or by the sponsor.)	
11. DOCUMENT AVAILABILITY (Any limitations on further dissemination of the document, other than those imposed by security classification.) Unlimited			
12. DOCUMENT ANNOUNCEMENT (Any limitation to the bibliographic announcement of this document. This will normally correspond to the Document Availability (11). However, where further distribution (beyond the audience specified in (11) is possible, a wider announcement audience may be selected.) Unlimited			

13. **ABSTRACT** (A brief and factual summary of the document. It may also appear elsewhere in the body of the document itself. It is highly desirable that the abstract of classified documents be unclassified. Each paragraph of the abstract shall begin with an indication of the security classification of the information in the paragraph (unless the document itself is unclassified) represented as (S), (C), (R), or (U). It is not necessary to include here abstracts in both official languages unless the text is bilingual.)

Validation of the computational electromagnetic code FACETS (Frequency Asymptotic Code for Electromagnetic Target Scattering) for simulating radar images of a target is obtained, through direct simulation-to-measurement comparisons. A 3-dimensional computer-aided design model of a canonical target known as SLICY (Sandia laboratory Implementation of Cylinders) and the corresponding measured SAR (Synthetic Aperture Radar) image data of SLICY from the MSTAR (Moving and Stationary Target Acquisition and Recognition) datasets are used in the validation process. Computed SAR images of the SLICY target sampled over 360 degrees in azimuth and at two elevation angles are evaluated by comparing against measured images. The results indicate that computed images of high fidelity can be generated if the scattering primitives on the target are correctly included in the computer-aided design model and this information is correctly translated for computation in the electromagnetic code.

14. **KEYWORDS, DESCRIPTORS or IDENTIFIERS** (Technically meaningful terms or short phrases that characterize a document and could be helpful in cataloguing the document. They should be selected so that no security classification is required. Identifiers, such as equipment model designation, trade name, military project code name, geographic location may also be included. If possible keywords should be selected from a published thesaurus, e.g. Thesaurus of Engineering and Scientific Terms (TEST) and that thesaurus identified. If it is not possible to select indexing terms which are Unclassified, the classification of each should be indicated as with the title.)

computational electromagnetic modelling, SLICY, Synthetic Aperture Radar, radar images, radar cross-section.

Defence R&D Canada

Canada's leader in Defence
and National Security
Science and Technology

R & D pour la défense Canada

Chef de file au Canada en matière
de science et de technologie pour
la défense et la sécurité nationale



www.drdc-rddc.gc.ca